# The Neural Bases of Egocentric Spatial Representation for Extracorporeal and Corporeal Tasks: An fMRI Study

Stephanie Leplaideur, Annelise Moulinet-Raillon, Quentin Duché, Lucie Chochina, Karim Jamal, Jean-Christophe Ferré, Elise Bannier, Isabelle Bonan

brain sciences

MDPI

*Article*

# The Neural Bases of Egocentric Spatial Representation for Extracorporeal and Corporeal Tasks: An fMRI Study

**Stephanie Leplaideur [1,2,3,*], Annelise Moulinet-Raillon [4], Quentin Duché [2], Lucie Chochina [3], Karim Jamal [1], Jean-Christophe Ferré [2,5], Elise Bannier [2,5,†] and Isabelle Bonan [1,2,†]**

1 Physical and Rehabilitation Medicine Department, Rennes University Hospital, 35000 Rennes, France; krmjamal@me.com (K.J.); isabelle.bonan@chu-rennes.fr (I.B.)
2 Univ Rennes, CNRS, Inria, Inserm, IRISA UMR 6074, Empenn ERL U 1228, 35000 Rennes, France; quentin.duche@irisa.fr (Q.D.); jean-christophe.ferre@chu-rennes.fr (J.-C.F.); elise.bannier@irisa.fr (E.B.)
3 Physical Medicine and Neurological Rehabilitation Department, Kerpape, 56270 Ploemeur, France; lucie.chochina@mutualite29-56.fr
4 Department of Physical and Rehabilitation Medicine, Duchenne Hospital, 62200 Boulogne sur Mer, France; anneliseraillon@yahoo.fr
5 Radiology Department, Rennes University Hospital, 35000 Rennes, France
* Correspondence: stephanie.leplaideur@chu-rennes.fr; Tel.: +33-299-284-218
† Both authors contributed equally to this work.

**Abstract:** (1) Background: Humans use reference frames to elaborate the spatial representations needed for all space-oriented behaviors such as postural control, walking, or grasping. We investigated the neural bases of two egocentric tasks: the extracorporeal subjective straight-ahead task (SSA) and the corporeal subjective longitudinal body plane task (SLB) in healthy participants using functional magnetic resonance imaging (fMRI). This work was an ancillary part of a study involving stroke patients. (2) Methods: Seventeen healthy participants underwent a 3T fMRI examination. During the SSA, participants had to divide the extracorporeal space into two equal parts. During the SLB, they had to divide their body along the midsagittal plane. (3) Results: Both tasks elicited a parieto-occipital network encompassing the superior and inferior parietal lobules and lateral occipital cortex, with a right hemispheric dominance. Additionally, the SLB > SSA contrast revealed activations of the left angular and premotor cortices. These areas, involved in attention and motor imagery suggest a greater complexity of corporeal processes engaging body representation. (4) Conclusions: This was the first fMRI study to explore the SLB-related activity and its complementarity with the SSA. Our results pave the way for the exploration of spatial cognitive impairment in patients.

**Keywords:** spatial cognition; egocentric reference frame; functional MRI



**Citation:** Leplaideur, S.; Moulinet-Raillon, A.; Duché, Q.; Chochina, L.; Jamal, K.; Ferré, J.-C.; Bannier, E.; Bonan, I. The Neural Bases of Egocentric Spatial Representation for Extracorporeal and Corporeal Tasks: An fMRI Study. *Brain Sci.* **2021**, *11*, 963. https://doi.org/10.3390/brainsci11080963

Academic Editors: Arnaud Saj and Roberta Ronchi

Received: 27 May 2021
Accepted: 19 July 2021
Published: 22 July 2021



## 1. Introduction

Multiple sources of afferent information (from vestibular, visual, and proprioceptive receptors) and efferent information (from motor effectors) are needed to elaborate internal spatial representations of the body in space [1,2]. These inputs can be integrated into different and changing systems of coordinates, depending on the person's position in space and the nature of the task. The egocentric reference frame encodes spatial information centered on body coordinates [3–8]. This frame involves two spatial components, depending on the intended action: extracorporeal and corporeal [9]. The extracorporeal component enables individuals to locate stimuli perceived in the extrapersonal space relative to their body and orient their actions in the environment. The corporeal component allows individuals to elaborate personal representations of the location and configuration of their body centered in space, in order to perform tasks such as personal care [4,10]. Two tasks have been used to explore these egocentric reference frames: the subjective straight-ahead task (SSA) and, more recently, the subjective longitudinal body plane task (SLB). The SSA explores extracorporeal space perception centered on the body. Participants

imagine a plane starting from their midsagittal body and going straight ahead, dividing the extracorporeal space into two parts [4,10,11]. In the SLB, participants are asked to divide their corporeal space into two parts. They indicate with a button press when the bar virtually divided their corporeal space into two equal parts along their body's midsagittal plane [5,11–14]. There are well-known clinical differences between extracorporeal and corporeal tasks [5,12], and the integration of relevant information can be differentially affected following brain damage [15]. For example, differences between extracorporeal and corporeal abilities have been identified when assessing unilateral spatial neglect. An impact of body representation in space on asymmetrical postural behaviors has also been reported. One previous study highlighted a strong relationship between SLB disturbance and postural asymmetry in patients with chronic stroke [5]. However, the neural basis of these differences has never been investigated. It is essential to improve knowledge in this field, as gaining a better understanding of the mechanisms involved in elaborating the egocentric reference frame would inform rehabilitation strategies for patients with spatial cognition disorders following stroke.

The present work was the first to use fMRI to study the commonalities and differences in brain activity between two egocentric tasks involving either extracorporeal or corporeal space. We hypothesized that both tasks would activate a bilateral fronto-parieto-occipital network, especially the posterior parietal and premotor cortices, with right hemispheric predominance [15–18]. Moreover, we expected the two tasks to activate distinct subregions of the network. This research among healthy participants was an ancillary study to a multicenter study exploring spatial cognitive disorders in patients with stroke.

## 2. Materials and Methods

### *2.1. Participants*

We included 17 healthy volunteers (7 men and 10 women: Mean age = 50.4 years, SD = 14.9, range 23–70). They were all right handed on their declaration. All participants gave their written informed consent to take part in this study, which was approved by the Poitiers-France III West institutional review board (no. 05/12/16; AVCPOSTIM study—clinical trial identifier NCT01677091). Exclusion criteria were (1) contraindication to magnetic field exposure, (2) neurological disease, and (3) history of balance disorders. All participants had normal or corrected-to-normal vision.

### *2.2. Experimental Design*

The SSA and SLB tasks were performed in a supine position in an MRI scanner. For the SSA task, participants were instructed to divide the extracorporeal space in front of them into two halves [5,10,12,19]. A vertical green bar scanned the black screen from left to right and from right to left, with different random starting positions within the range of −7° to +7°, at a speed of 2° per second [20]. The instruction was "Press the button when the bar is straight ahead and divides the space in front of you into two equal parts" (Figure 1 and Supplementary File S1).

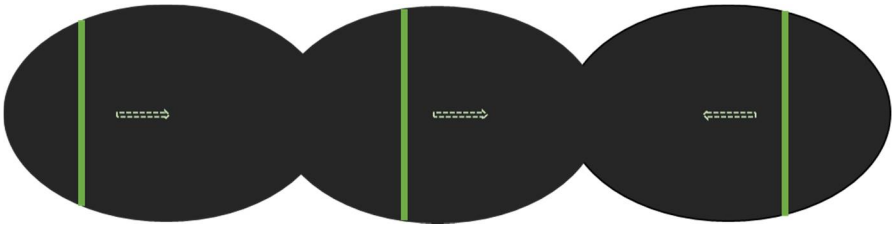

**Figure 1.** Schematic diagram of the subjective straight-ahead (SSA) fMRI task. Dotted arrows represent the direction of motion.

During the SLB task, a green bar moved along the plane orthogonal to the line going through the navel [5,13,21]. The bar rotated alternately leftward and rightward, with different random starting angles within the range of −30°/+30°, at a speed of 2° per

second. The instruction was "Press the button when the bar is aligned with a virtual plane dividing your corporeal space into two equal parts" (Figure 2 and Supplementary File S2).

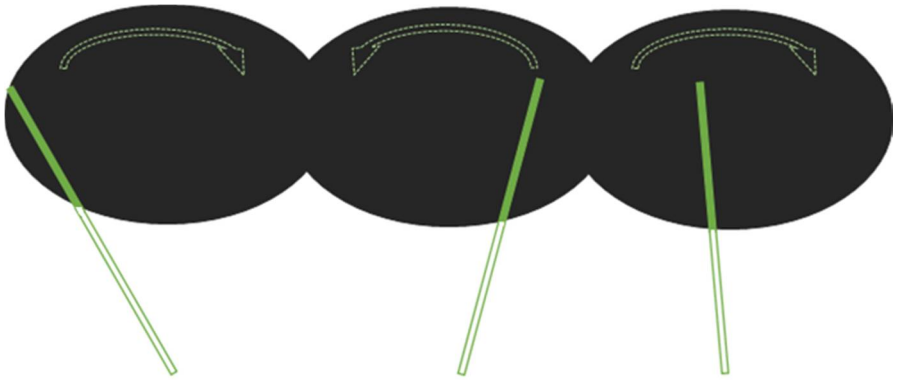

**Figure 2.** Schematic diagram of the subjective longitudinal body fMRI task. The dotted arrow represents the bar's motion. The empty bars represent the virtual continuous plane centered on the navel.

During the control condition, the same sequence of bar movements was presented, but participants were instructed to press the button when the bar changed direction.

Each fMRI sequence lasted 3 min and followed a block design: 30 s blocks of task and 30 s block of control conditions. In each block, the bar passed through the center six times at a constant speed of two degrees per second [20]. The process is similar for both tasks. The tasks were implemented using E-Prime 2.0 Professional software (Psychology Software Tools, Pittsburgh, PA, USA) and presented using goggles (NordicNeuroLab, Bergen, Norway) attached to the head coil to immerse participants in the task without any spatial clues. The instruction was presented via the goggles just before the task, in different colors for task and rest at the beginning of each block. To perform the tasks, participants reported their perception by pressing a button with their right index finger. Before the experiment, they practiced outside the scanner until they were able to perform the tasks. They all confirmed they understood the instructions. The difference between target identification (respectively, straight ahead or longitudinal axis) and button press time were computed both for SSA and SLB tasks.

### *2.3. MRI Acquisition*

MRI acquisition was performed on a 3 tesla scanner (Magnetom Verio; Siemens Medical Solutions, Erlangen, Germany) with a 12-channel head coil. The alignment of head, shoulders, trunk, and limbs was checked by the experimenter before MRI acquisition. The head and the trunk were maintained with foam pads.

The following MR sequences were acquired:

- sagittal morphological isotropic 3D T1 MPRAGE sequence (repetition time (TR)/inversion time (TI)/echo time (TE): 1900/900/2.26 ms, field of view (FOV) 256 × 256 $mm^2$, 160 slices, 1 × 1 × 1 $mm^3$ voxel size);
- field map with two echo times for distortion correction; and
- two blood oxygen level dependent (BOLD) fMRI sequences using a single-shot T2*-weighted EPI sequence (TR/TE: 3000/36 ms, 210 × 210 $mm^2$, FOV, 2 × 2 × 4 $mm^3$, voxel size, 24 slices). Interleaved slices were acquired parallel to the anterior commissure posterior commissure line with no gap.

In total, the experiment was completed in 15 min.

Images were preprocessed and analyzed using Statistical Parametric Mapping (SPM12; Wellcome Department of Imaging Neuroscience, University College London, London, UK [22]; revision 7487) implemented in MATLAB. Morphological images were segmented, corrected for bias, and normalized to Montreal Neurological Institute atlas space (MNI).

Slice timing, spatial realignment, distortion correction, coregistration to the morphological images, and normalization were applied, followed by 6 mm full width at half maximum (FWHM) isotropic Gaussian kernel smoothing. The canonical hemodynamic response function and its temporal derivative were used for model estimation, and three contrasts were evaluated: "SSA > control condition", "SLB > control condition", and "SLB > SSA".

### *2.4. Statistical Modeling and Inference Analysis*

Given that a large number of regions of interest are reported in the literature, we ran voxelwise analyses across the whole brain. A cluster extent of 25 voxels was determined by running a Monte Carlo simulation [23–25] using cluster threshold betas based on an individual voxel threshold of $p = 0.001$ and a corrected threshold of $p = 0.05$. The two tasks were compared using a paired t test with a cluster extent of 25 voxels.

To allow us to compare our results with those of previous studies [4,7,20,26–29], we converted the literature data into MNI coordinates using the MNI to Talairach application [30,31]. We visualized our results using SPM12 and the xjView toolbox (available online: https://www.alivelearn.net/xjview (accessed on 27 May 2021) and MRIcroGL (available online: https://www.mccauslandcenter.sc.edu/mricrogl/ (accessed on 27 May 2021). The interpretation was performed in MNI space, using the automated anatomical labeling atlas (AAL3) [32], Jülich brain cytoarchitectonic atlas [33–36], and brainnetome atlas [37] for cyto-myelo labeling. The latter, based on anatomical connectivity parcellation and containing 246 regions of the bilateral hemispheres (210 cortical and 36 subcortical subregions), was the most useful one for identifying activated regions reported in the results.

## 3. Results

Subjects responded within the standard to both tasks showing the reliability of the tasks. The SSA mean deviation was −0.4°, SD 1.3; the SLB mean deviation was −1°, SD 0.3. The mean response times of both tasks were not significantly different suggesting a similar complexity ($p = 1.17$).

### *3.1. Subjective Straight-Ahead Task (SSA)*

The "SSA > control condition" contrast highlighted a parieto-occipital network shown in in Figure 3 and Table 1. We observed right-hemispheric dominance (74.3% of activated voxels).

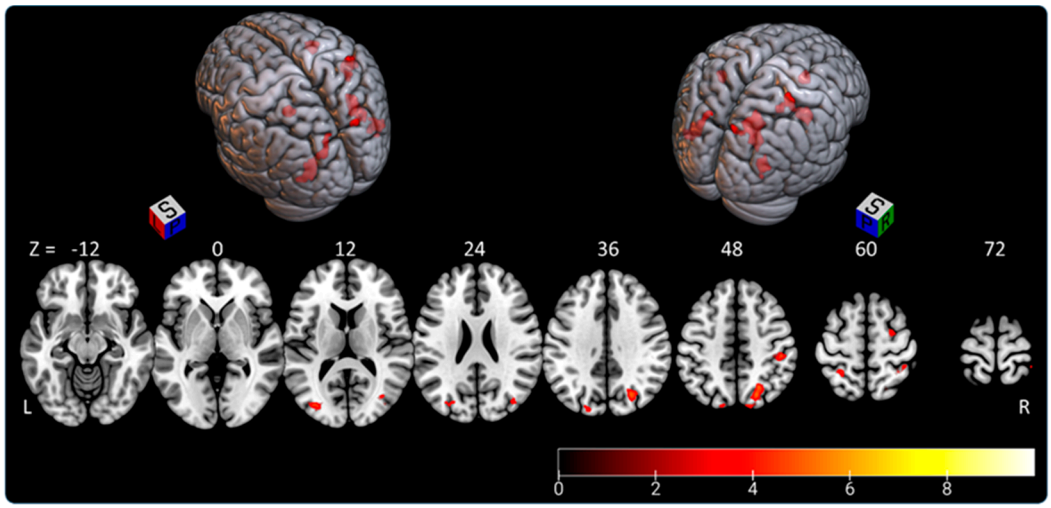


**Figure 3.** Rendered image of activated clusters highlighted by the "SSA > control condition" contrast. The color bar indicates *t*-values (BOLD); L—left, P—posterior, R—right, S—superior, Z coordinates in MNI atlas.

**Table 1.** Activated areas highlighted by the "SSA > control condition" contrast. The number of voxels is given for each cluster, together with the side (i.e., left or right hemisphere), the cluster composition (i.e., percentage of voxels in each area assigned using AAL3 and brainnetome atlas), MNI coordinates and t value of the peak. Only activated areas covering more than 10% of the cluster are shown.

| Cluster Voxels/Side | AAL3 % in the Area | Peak MNI Coordinates (x y z)/T Value | Brainnetome % in the Area |
|---|---|---|---|
| 226/right | 42.5 occipital sup<br>33.6 parietal sup | 24 −62 46/5.630 | 31.9 lsOccg<br>28.8 A7c |
| 92/left | 96.7 occipital mid | −30 −84 14/5.023 | 44.6 mOccG<br>35.9 A39c |
| 81/right | 61.7 postcentral<br>29.6 supramarginal | 46 −28 42/5.440 | 69.1 A40rd<br>19.8 A2 |
| 66/right | 87.9 occipital mind | 42 −80 18/5.471 | 54.5 A39c<br>31.8 mOccG |
| 58/right | 55.2 postcentral<br>25.9 parietal inf<br>19.0 parietal sup | 38 −44 66/5.216 | 12.1 A7pc<br>60.3 A5l<br>19.0 A7ip |
| 40/right | 72.5 frontal sup<br>17.5 precentral | 26 −4 58/5.087 | 85.0 A6cdl<br>10.0 A6dl |
| 39/left | 76.9 occipital sup<br>23.1 parietal sup | −18 −86 38/4.506 | 10.3 msOccG<br>79.5 lsOccG |
| 31/left | 51.6 parietal sup<br>25.8 parietal inf<br>22.6 postcentral | −26 −46 58/6.259 | 19.4 A7pc<br>38.7 A5l |

The activated voxels in the eight significant clusters were distributed as follows:

- the right parietal lobe (superior parietal lobule: A7c, A5l, A7pc; inferior parietal lobule: A39c, A40rd, A40rv; precuneus: dmPOS; postcentral gyrus: A2) representing 45.5% of activated areas;
- the right lateral occipital cortex (msOccG, lsOccG, mOccG), representing 21.5% of activated areas;
- the left lateral occipital cortex (V5/MT+, msOccG, lsOccG, mOccG), representing 16% of activated areas;
- the left parietal lobe (superior parietal lobule: A5l, A7pc; and inferior parietal lobule: A39c), representing 9.5% of activated areas; and
- the right premotor cortex (superior frontal gyrus: A6cdl), representing 7.5% of activated areas.

### *3.2. Subjective Longitudinal Body Plane Task (SLB)*

The "SLB > control condition" contrast highlighted a fronto-parieto-occipital network extending to the temporal lobe and insula, with right-hemispheric predominance (75.5% of clusters located in right hemisphere). Activated clusters are shown in Figure 4 and Table 2.

Activated voxels were distributed as follows:

- the right parietal lobe (superior parietal lobule: A7r, A7c, A5l, A7pc, A7ip; inferior parietal lobule: A39c, A40rd, A40rv; precuneus: dmPOS; postcentral gyrus: A1/2/3ulhf, A2, A1/2/3tru), representing 27% of activated areas;
- the right lateral occipital cortex (V5/M+, msOccG, lsOccG, mOccG, iOccG), representing 22.5% of activated areas;
- the right frontal lobe (predominant in the precentral gyrus: A4hf, A6cdl, A4ul, A4tl, A6cvl; superior frontal gyrus: A8m, A6dl, A6m; inferior frontal gyrus: A44d, A44op; paracentral gyrus: A4ll), representing 21% of activated areas;

- the left lateral occipital cortex (V5/MT+, mOccG, iOccG), representing 8% of activated areas;
- the left frontal lobe (supplementary motor area: A6m; precentral gyrus: A4hf, A6cdl, A4ul, A4t; and paracentral lobule: A4ll), representing 7.5% of activated areas; and
- less than 5% in each of the following areas: left parietal lobe (superior parietal lobule: A5l, A7pc; inferior parietal lobule: A39c, A39rv; postcentral gyrus: A1/2/3ulhf, A2), right insular lobe (vIa, dIa, dIg, dId), left temporal lobe (middle temporal gyrus: A37dl; inferior temporal gyrus: A37vl; fusiform gyrus: A37lv), left cingulate gyrus, right temporal lobe (middle temporal gyrus: A37dl; inferior temporal gyrus: A37vl; fusiform gyrus: A37lv), and right cingulate gyrus.

**Table 2.** Activated areas highlighted by "SLB > control condition" contrast. The number of voxels is given for each cluster, together with the side (i.e., left or right hemisphere), the cluster composition (i.e., the percentage of voxels in each area assigned using AAL3 and brainnetome atlas), MNI coordinates and t value of the peak. Only activated areas covering more than 10% of the cluster are shown.

| Cluster Voxels/Side | AAL3 % in the Area | Peak MNI Coordinates (x y z)/T Value | Brainnetome % in the Area |
|---|---|---|---|
| 565/right | 25.3 occipital mid<br>25.1 temporal mid<br>18.9 occipital sup<br>13.3 temporal inf | 44 −66 −6/10.448 | 16.6 mOccG<br>9.7 msOccG<br>8.5 lsOccG<br>38.1 V5/MT+ |
| 512/right | 59.4 postcentral<br>16.8 supramarginal<br>15.0 parietal sup | 50 −22 42/6.4996 | 18.8 A2<br>24.2 A40rd<br>15.4 A5l<br>11.1 A40rv |
| 240/right | 64.6 frontal sup<br>15.0 precentral<br>11.3 frontal mid | 36 −6 58/6.921 | 56.3 A6cdl<br>22.5 A6dl |
| 218/left | 59.2 occipital mid<br>20.2 temporal mid<br>18.4 occipital inf | −34 −78 10/6.0758 | 19.7 mOccG<br>45.4 V5/MT+<br>11.0 A39c |
| 152/right-left | 59.9 supp motor area L<br>31.6 sup motor area R | −4 −12 58/6.0816 | 51.3 lA6m<br>26.3 rA6m |
| 107/right | 60.8 frontal inf oper<br>39.3 precentral | 58 12 30/6.2155 | 92.5 A6cvl |
| 78/right | 87.2 insula | 44 20 −6/5.5758 | 34.6 dla<br>44.9 dld<br>11.5 A44op |
| 55/left | 98.2 precentral | −40 −10 66/5.086 | 45.5 A6cdl<br>29.1 A4hf<br>18.2 A4ul |
| 52/left | 73.1 postcentral<br>26.9 parietal sup | −40 −44 62/4.699 | 36.5 A7pc<br>38.5 A5l<br>19.2 A2 |
| 45/right-left | 53.3 cingulate mid L<br>31.1 cingulate mid R<br>11.1 sup motor area L | −2 6 42/6.001 | 57.8 lA24cd<br>35.6 rA24cd |
| 31/left | 51.6 postcentral<br>48.4 precentral | −38 −18 46/5.1726 | 38.7 A1/2/3ulhf<br>41.9 A4hf |

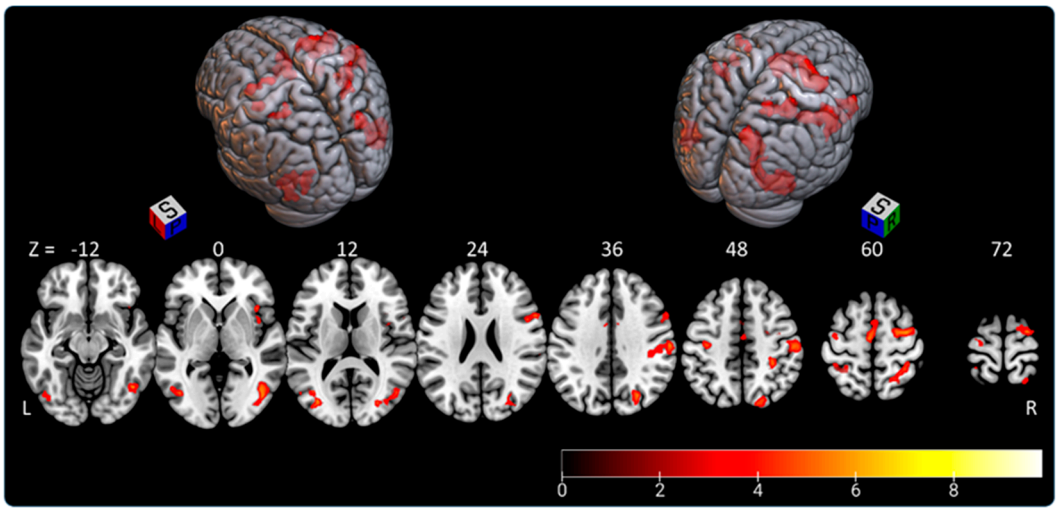


**Figure 4.** Rendered image of activated clusters highlighted by "SLB > control condition" contrast. The color bar indicates *t*-values (BOLD); L—left, P—posterior, R—right, S—superior, Z—coordinates in MNI atlas.

### *3.3. Subjective Longitudinal Body Plane Task versus Subjective Straight-Ahead Task*

Subjects responded within the standard to both tasks showing the reliability of the tasks. The SSA mean deviation was −0.4°, SD 1.3; the SLB mean deviation was −1°, SD 0.3. The mean response times of both tasks were not significantly different suggesting a similar complexity ($p$ = 1.17).

Both tasks elicited a parieto-occipital network that encompassed the superior and inferior parietal lobules, precuneus, and lateral occipital cortex. The "SLB > SSA" comparison revealed a larger activation area (2055 vs. 633 voxels) and higher intensity for the SLB task than for the SSA task. Moreover, the "SLB > SSA" contrast revealed activation in the left angular and precentral gyri (Figure 5, Table 3).

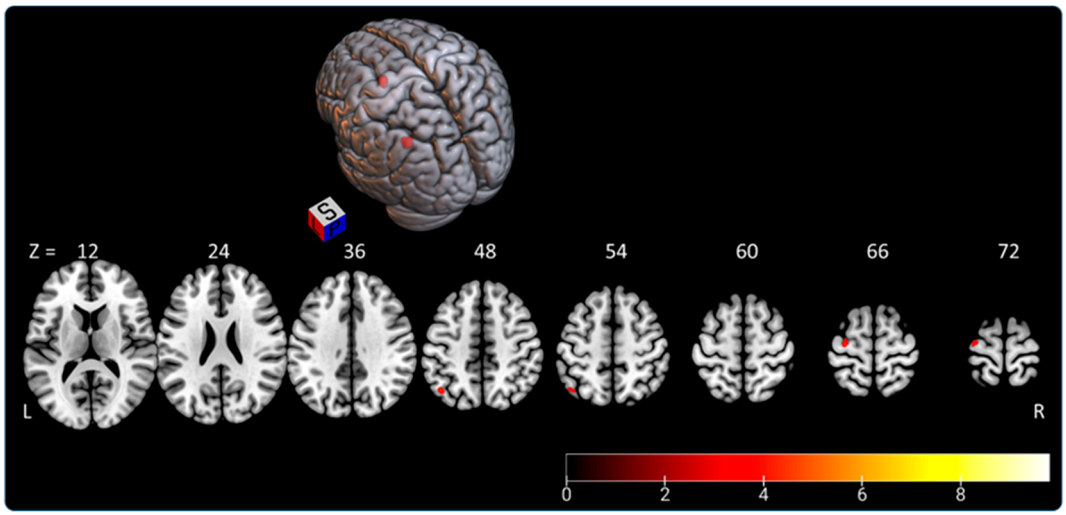


**Figure 5.** Rendered image of activated clusters highlighted by "SLB > SSA" contrast. The color bar indicates *t*-values (BOLD); L—left, P—posterior, R—right, S—superior, Z coordinates in MNI atlas.

**Table 3.** Activated areas highlighted by "SLB > SSA" contrast. The number of voxels is given for each cluster, together with the side (i.e., left or right hemisphere), the cluster composition (i.e., the percentage of voxels in each area assigned using AAL3 and brainnetome atlas), MNI coordinates and t value of the peak. Only activated areas covering more than 10% of the cluster are shown.

| Cluster Voxels/Side | AAL3 % in the Area | PeakMNI Coordinates (x y z)/T Value | Brainnetome % in the Area |
|---|---|---|---|
| 28/left | 71.0 angular<br>7.1 parietal inf | −44 −66 50/4.9301 | 57.1 A39rd<br>7.1 A39rv |
| 25/left | 92.0 precentral | −30 −14 70/6.430 | 52.0 A6cdl<br>40.0 A4ul |

## 4. Discussion

Using fMRI, the present study investigated the neural bases of processes elicited by two different egocentric tasks in healthy participants: SSA and SLB. This was the first time that the SLB task had been implemented in fMRI, reproducing the clinical assessment setting in a supine position without visual clues. We demonstrated its feasibility and complementarity with the SSA task [20]. These tasks can both be administered to patients with spatial cognitive disorders following stroke. Our results will enhance understanding of the egocentric reference frame concept both in healthy participants and in patients with a brain lesion.

The SSA and SLB both activated a parieto-occipital network with right-hemispheric predominance. This is in agreement with previous human and animal studies reporting activation of a fronto-parieto-occipital network by spatial cognition tasks [3,4,7,20,26–29,38–40]. Studies in nonhuman primates have highlighted the involvement of the posterior parietal cortex, parieto-insular vestibular cortex, and parieto-occipital sulcus as multimodal integration areas [38–46]. In 2010, Galati et al. published a review of studies investigating egocentric and allocentric tasks in healthy participants. This review, similar to more recent articles in humans [4,7,18,20,26–29], described the crucial role of the bilateral fronto-parietal network for spatial tasks, with involvement of the posterior parietal cortex extending to the superior frontal region [7,20,27,29]. In particular, egocentric activity was related to the posterior parietal cortex including the precuneus [27,29], superior parietal lobule [7,20,27,28], and intraparietal sulcus [20]. In the right hemisphere, activation maps often extend to the supramarginalis gyrus and angular gyrus [7,20,27]. These areas involved in the integration and selection of multimodal sensory inputs may, therefore, support the elaboration of mental representations of the body in space [8,20]. Activated areas reported in the superior and inferior parietal lobules confirm the involvement of somesthesis and motor imagery in the egocentric reference frame.

We found strong activity in the right lateral occipital cortex implicated in visual perception, corroborating previous experimental findings [43]. As we used a moving bar instead of a static image, the motion may have increased occipital activity.

Along these lines, we found less extensive frontal activation in the superior and inferior frontal gyri than in previous studies [27,29]. However, these studies compared an egocentric task with an allocentric task in the same run. As the background required to perform the allocentric task is similar in both the SSA and SLB conditions, participants may engage attention and inhibition functions in order to be able to shift between the two tasks, thereby, increasing cognitive load and thus prefrontal activity. This may explain the lack of prefrontal activity in our study, in which we used a separate background for each task.

By analyzing and comparing two tasks involving the egocentric reference frame, our study represents a milestone in the comprehension of egocentric frame mechanisms. We found significant differences in fMRI activity between the corporeal and extracorporeal egocentric tasks. Interestingly, the SLB task activated additional areas in the left hemisphere, including the angular (A39rd, A39rv, A40c) and precentral gyrus (A6cdl, A4ul). The angular

gyrus is a high-level cognitive area involved in attentional and memory processes [47,48], whereas the premotor cortex is engaged in movement selection and preparation [49]. The left lateralization of premotor cortex activity during the SLB task can be viewed from the perspective of motor imagery tasks that typically activate the left premotor cortex [50–52]. This sheds light on the complexity of corporeal task processes. Moreover, the SLB task appears to require mental spatial coordinate transformation, as participants have to mentally align the external cues (the light bar) with their body's midsagittal plane [53]. This view is supported by studies showing the implication of left parietal temporal occipital junction lesions in body schema disturbances, causing difficulties in spatial orientation [47]. Moreover, our results are consistent with the hypothesis of a functional interhemispheric connection involved in egocentric processing, particularly during corporeal tasks [15].

The present study had several limitations. First, the sample size is small and increasing sample sizes are desired. However, previous studies have included even smaller samples (fewer than 10 participants). Moreover, the age range is wide, but we do not expect variability in healthy controls as regards this kind of task [54–56]. Indeed, age has been reported to affect allocentric tasks while preserving egocentric strategies. Furthermore, we did not observe any age effect on task performance. Second, we focused our investigation on the egocentric reference frame in particular. Given the lack of study on this subject, we aimed to improve knowledge of the elaboration of the egocentric reference frame. Thus, we implemented two egocentric tasks oriented toward corporal or extracorporeal spaces with a control condition when the bar changed direction. In order to verify how specific the MRI findings are in terms of brain processing of egocentricity, it would have been interesting to add an allocentric task and compare our results to previous works. Third, the 3 min runtime may have been too short to obtain reliable results. However, we used an AB block design to compensate for the short duration of the tasks, which was a requirement in this clinical setting involving patients with stroke.

## 5. Conclusions

This study investigated two egocentric tasks oriented toward either extracorporeal or corporeal spaces in 17 healthy participants. There was a large overlap between the SSA and SLB tasks, with a right fronto-parieto-occipital pattern of activity, showing that they share a common network. However, the SLB task elicited additional activity in the left angular gyrus and premotor cortex, suggesting greater complexity for SLB processes with functional interhemispheric connectivity. These results shedding light on the clinical dissociations reported for spatial cognitive disorders need to be confirmed in studies involving patients with spatial cognition disorders.

**Supplementary Materials:** The following are available online at https://www.mdpi.com/article/10.3390/brainsci11080963/s1, File S1. Video of part of SSA in fMRI (gif). File S2. Video of part of SLB in fMRI (gif).

**Author Contributions:** Conceptualization, S.L., A.M.-R., L.C., E.B., and I.B.; data curation, E.B.; formal analysis, S.L., J.-C.F., E.B., and I.B.; funding acquisition, A.M.-R. and I.B.; investigation, S.L., A.M.-R., L.C., and K.J.; methodology, S.L., A.M.-R., Q.D., J.-C.F., E.B., and I.B.; software, Q.D.; supervision, E.B. and I.B.; writing—original draft, S.L. and A.M.-R.; writing—review and editing, S.L., E.B., and I.B. All authors have read and agreed to the published version of the manuscript.

**Funding:** This study was supported by grants from "la fondation de l'avenir" and the French Ministry of Health (PHRC AVC POSTIM/2011/09.11).

**Institutional Review Board Statement:** The study was conducted according to the guidelines of the Declaration of Helsinki and approved by the Poitiers III West review Board (no. 05/12/16).

**Informed Consent Statement:** All participants gave their informed consent to participate in the AVCPOSTIM study.

**Data Availability Statement:** The datasets used and analyzed during the current study are available from the corresponding author on request.

**Acknowledgments:** I would like to thank Assia Jaillard for providing insightful feedback and Cathy Stinear for her guidance and support. MRI data acquisitions were carried out in the Neurinfo MRI research facility of the University of Rennes I. Neurinfo is funded by the European Union (FEDER), French Government, Brittany regional Council, Rennes Metropole, INRIA, INSERM, and Rennes University Hospital.

**Conflicts of Interest:** The authors declare that they have no competing interests.

## References

1. Bonan, I.V.; Marquer, A.; Eskiizmirliler, S.; Yelnik, A.P.; Vidal, P.-P. Sensory Reweighting in Controls and Stroke Patients. *Clin. Neurophysiol.* **2013**, *124*, 713–722. [CrossRef] [PubMed]
2. Rode, G.; Pérennou, D.; Azouvi, P. Spatial Cognition. *Ann. Phys. Rehabil. Med.* **2017**, *60*, 123. [CrossRef] [PubMed]
3. Andersen, A.; Snyder, H. Coordinate Transformations in the Representation of Spatial Information. *Curr. Opin. Neurobiol.* **1993**, *3*, 171–176. [CrossRef]
4. Galati, G.; Pelle, G.; Berthoz, A.; Committeri, G. Multiple Reference Frames Used by the Human Brain for Spatial Perception and Memory. *Exp. Brain Res.* **2010**, *206*, 109–120. [CrossRef] [PubMed]
5. Jamal, K.; Leplaideur, S.; Rousseau, C.; Chochina, L.; Moulinet-Raillon, A.; Bonan, I. Disturbances of Spatial Reference Frame and Postural Asymmetry after a Chronic Stroke. *Exp. Brain Res.* **2018**, *236*, 2377–2385. [CrossRef]
6. Jeannerod, M.; Biguer, B. Egocentric reference and represented space. *Rev. Neurol.* **1989**, *145*, 635–639.
7. Saj, A.; Cojan, Y.; Musel, B.; Honoré, J.; Borel, L.; Vuilleumier, P. Functional Neuro-Anatomy of Egocentric versus Allocentric Space Representation. *Neurophysiol. Clin. Clin. Neurophysiol.* **2014**, *44*, 33–40. [CrossRef]
8. Ventre, J.; Flandrin, J.M.; Jeannerod, M. In Search for the Egocentric Reference. A Neurophysiological Hypothesis. *Neuropsychologia* **1984**, *22*, 797–806. [CrossRef]
9. Zipser, D.; Andersen, R.A. A Back-Propagation Programmed Network That Simulates Response Properties of a Subset of Posterior Parietal Neurons. *Nature* **1988**, *331*, 679–684. [CrossRef]
10. Chokron, S.; Colliot, P.; Atzeni, T.; Bartolomeo, P.; Ohlmann, T. Active versus Passive Proprioceptive Straight-Ahead Pointing in Normal Subjects. *Brain Cogn.* **2004**, *55*, 290–294. [CrossRef]
11. Bartolomeo, P. Egocentric Frame of Reference: Its Role in Spatial Biasafter Right Hemisphere Lesions. *Neuropsychologia* **1999**, *37*, 881–894. [CrossRef]
12. Rousseaux, M.; Honoré, J.; Saj, A. Body Representations and Brain Damage. *Neurophysiol. Clin. Clin. Neurophysiol.* **2014**, *44*, 59–67. [CrossRef]
13. Barra, J.; Chauvineau, V.; Ohlmann, T.; Gresty, M.; Perennou, D. Perception of Longitudinal Body Axis in Patients with Stroke: A Pilot Study. *J. Neurol. Neurosurg. Psychiatry* **2007**, *78*, 43–48. [CrossRef]
14. Barra, J.; Benaim, C.; Chauvineau, V.; Ohlmann, T.; Gresty, M.; Pérennou, D. Are Rotations in Perceived Visual Vertical and Body Axis after Stroke Caused by the Same Mechanism? *Stroke* **2008**, *39*, 3099–3101. [CrossRef]
15. Committeri, G.; Pitzalis, S.; Galati, G.; Patria, F.; Pelle, G.; Sabatini, U.; Castriota-Scanderbeg, A.; Piccardi, L.; Guariglia, C.; Pizzamiglio, L. Neural Bases of Personal and Extrapersonal Neglect in Humans. *Brain* **2007**, *130*, 431–441. [CrossRef] [PubMed]
16. Caggiano, P.; Jehkonen, M. The 'Neglected' Personal Neglect. *Neuropsychol. Rev.* **2018**, *28*, 417–435. [CrossRef] [PubMed]
17. Ten Brink, A.F.; Biesbroek, J.M.; Oort, Q.; Visser-Meily, J.M.A.; Nijboer, T.C.W. Peripersonal and Extrapersonal Visuospatial Neglect in Different Frames of Reference: A Brain Lesion-Symptom Mapping Study. *Behav. Brain Res.* **2019**, *356*, 504–515. [CrossRef] [PubMed]
18. Ruotolo, F.; Ruggiero, G.; Raemaekers, M.; Iachini, T.; van der Ham, I.J.M.; Fracasso, A.; Postma, A. Neural Correlates of Egocentric and Allocentric Frames of Reference Combined with Metric and Non-Metric Spatial Relations. *Neuroscience* **2019**, *409*, 235–252. [CrossRef] [PubMed]
19. Richard, C.; Honore, J.; Bernati, T.; Rousseaux, M. Straight-Ahead Pointing Correlates with Long-Line Bisection in Neglect Patients. *Cortex* **2004**, *40*, 75–83. [CrossRef]
20. Vallar, G.; Lobel, E.; Galati, G.; Berthoz, A.; Pizzamiglio, L.; Le Bihan, D. A Fronto-Parietal System for Computing the Egocentric Spatial Frame of Reference in Humans. *Exp. Brain Res.* **1999**, *124*, 281–286. [CrossRef] [PubMed]
21. Barra, J.; Oujamaa, L.; Chauvineau, V.; Rougier, P.; Perennou, D. Asymmetric Standing Posture after Stroke Is Related to a Biased Egocentric Coordinate System. *Neurology* **2009**, *72*, 1582–1587. [CrossRef] [PubMed]
22. Penny, W.; Friston, K.; Ashburner, J.; Kiebel, S.; Nichols, T. *Statistical Parametric Mapping: The Analysis of Functional Brain Images*, 1st ed.; Academic Press: Cambridge, MA, USA, 2006. Available online: https://www.elsevier.com/books/statistical-parametric-mapping-the-analysis-of-functional-brain-images/penny/978-0-12-372560-8 (accessed on 13 January 2020).
23. Boxerman, J.L.; Bandettini, P.A.; Kwong, K.K.; Baker, J.R.; Davis, T.L.; Rosen, B.R.; Weisskoff, R.M. The Intravascular Contribution to Fmri Signal Change: Monte Carlo Modeling and Diffusion-Weighted Studies in Vivo. *Magn. Reson. Med.* **1995**, *34*, 4–10. [CrossRef] [PubMed]

24. Slotnick, S.D. Resting-State FMRI Data Reflects Default Network Activity Rather than Null Data: A Defense of Commonly Employed Methods to Correct for Multiple Comparisons. *Cogn. Neurosci.* **2017**, *8*, 141–143. [CrossRef]
25. Slotnick, S.D. Cluster Success: FMRI Inferences for Spatial Extent Have Acceptable False-Positive Rates. *Cogn. Neurosci.* **2017**, *8*, 150–155. [CrossRef]
26. Galati, G.; Committeri, G.; Sanes, J.N.; Pizzamiglio, L. Spatial Coding of Visual and Somatic Sensory Information in Body-Centred Coordinates: Body-Centred Spatial Coding of Multimodal Stimuli. *Eur. J. Neurosci.* **2001**, *14*, 737–746. [CrossRef]
27. Galati, G.; Lobel, E.; Vallar, G.; Berthoz, A.; Pizzamiglio, L.; Le Bihan, D. The Neural Basis of Egocentric and Allocentric Coding of Space in Humans: A Functional Magnetic Resonance Study. *Exp. Brain Res.* **2000**, *133*, 156–164. [CrossRef]
28. Neggers, S.F.W.; Van der Lubbe, R.H.J.; Ramsey, N.F.; Postma, A. Interactions between Ego- and Allocentric Neuronal Representations of Space. *NeuroImage* **2006**, *31*, 320–331. [CrossRef]
29. Zaehle, T.; Jordan, K.; Wüstenberg, T.; Baudewig, J.; Dechent, P.; Mast, F.W. The Neural Basis of the Egocentric and Allocentric Spatial Frame of Reference. *Brain Res.* **2007**, *1137*, 92–103. [CrossRef] [PubMed]
30. Lacadie, C.M.; Fulbright, R.K.; Constable, R.T.; Papademetris, X. More Accurate Talairach Coordinates for NeuroImaging Using Nonlinear Registration. *NeuroImage* **2008**, *42*, 717–725. [CrossRef] [PubMed]
31. Talairach, J.; Tournoux, P. *Co-Planar Stereotaxic Atlas of the Human Brain*; Thieme: New York, NY, USA, 1988. Available online: https://www.thieme.com/books-main/neurosurgery/product/414-co-planar-stereotaxic-atlas-of-the-human-brain (accessed on 10 January 2020).
32. Rolls, E.T.; Huang, C.-C.; Lin, C.-P.; Feng, J.; Joliot, M. Automated Anatomical Labelling Atlas 3. *NeuroImage* **2020**, *206*, 116189. [CrossRef] [PubMed]
33. Amunts, K.; Schleicher, A.; Zilles, K. Cytoarchitecture of the Cerebral Cortex—More than Localization. *NeuroImage* **2007**, *37*, 1061–1065. [CrossRef] [PubMed]
34. Amunts, K.; Zilles, K. Architectonic Mapping of the Human Brain beyond Brodmann. *Neuron* **2015**, *88*, 1086–1107. [CrossRef] [PubMed]
35. Tzourio-Mazoyer, N.; Landeau, B.; Papathanassiou, D.; Crivello, F.; Etard, O.; Delcroix, N.; Mazoyer, B.; Joliot, M. Automated Anatomical Labeling of Activations in SPM Using a Macroscopic Anatomical Parcellation of the MNI MRI Single-Subject Brain. *NeuroImage* **2002**, *15*, 273–289. [CrossRef] [PubMed]
36. Zilles, K.; Amunts, K. Centenary of Brodmann's Map—Conception and Fate. *Nat. Rev. Neurosci.* **2010**, *11*, 139–145. [CrossRef]
37. Fan, L.; Li, H.; Zhuo, J.; Zhang, Y.; Wang, J.; Chen, L.; Yang, Z.; Chu, C.; Xie, S.; Laird, A.R.; et al. The Human Brainnetome Atlas: A New Brain Atlas Based on Connectional Architecture. *Cereb. Cortex* **2016**, *26*, 3508–3526. [CrossRef]
38. Andersen, R.A. Multimodal Integration for the Representation of Space in the Posterior Parietal Cortex. *Philos. Trans. R. Soc. B Lond. Biol. Sci.* **1997**, *352*, 1421–1428. [CrossRef]
39. Duhamel, J.-R.; Bremmer, F.; Ben Hamed, S.; Graf, W. Spatial Invariance of Visual Receptive Fields in Parietal Cortex Neurons. *Nature* **1997**, *389*, 845–848. [CrossRef]
40. Genovesio, A.; Ferraina, S. Integration of Retinal Disparity and Fixation-Distance Related Signals toward an Egocentric Coding of Distance in the Posterior Parietal Cortex of Primates. *J. Neurophysiol.* **2004**, *91*, 2670–2684. [CrossRef] [PubMed]
41. Chen, X.; DeAngelis, G.C.; Angelaki, D.E. Flexible Egocentric and Allocentric Representations of Heading Signals in Parietal Cortex. *Proc. Natl. Acad. Sci. USA* **2018**, *115*, E3305–E3312. [CrossRef]
42. Evrard, H.C. The Organization of the Primate Insular Cortex. *Front. Neuroanat.* **2019**, *13*, 43. [CrossRef] [PubMed]
43. Galletti, C.; Battaglini, P.P.; Fattori, P. Parietal Neurons Encoding Spatial Locations in Craniotopic Coordinates. *Exp. Brain Res.* **1993**, *96*, 221–229. [CrossRef] [PubMed]
44. Grüsser, O.J.; Pause, M.; Schreiter, U. Localization and Responses of Neurones in the Parieto-Insular Vestibular Cortex of Awake Monkeys (Macaca Fascicularis). *J. Physiol.* **1990**, *430*, 537–557. [CrossRef]
45. O'Keefe, J. Place Units in the Hippocampus of the Freely Moving Rat. *Exp. Neurol.* **1976**, *51*, 78–109. [CrossRef]
46. Schneider, R.J.; Friedman, D.P.; Mishkin, M. A Modality-Specific Somatosensory Area within the Insula of the Rhesus Monkey. *Brain Res.* **1993**, *621*, 116–120. [CrossRef]
47. Zacks, J.; Rypma, B.; Gabrieli, J.D.E.; Tversky, B.; Glover, G.H. Imagined Transformations of Bodies: An FMRI Investigation. *Neuropsychologia* **1999**, *37*, 1029–1040. [CrossRef]
48. Seghier, M.L. The Angular Gyrus: Multiple Functions and Multiple Subdivisions. *Neuroscientist* **2013**, *19*, 43–61. [CrossRef]
49. Rushworth, M.F.S.; Johansen-Berg, H.; Göbel, S.M.; Devlin, J.T. The Left Parietal and Premotor Cortices: Motor Attention and Selection. *NeuroImage* **2003**, *20*, S89–S100. [CrossRef]
50. Hétu, S.; Grégoire, M.; Saimpont, A.; Coll, M.-P.; Eugène, F.; Michon, P.-E.; Jackson, P.L. The Neural Network of Motor Imagery: An ALE Meta-Analysis. *Neurosci. Biobehav. Rev.* **2013**, *37*, 930–949. [CrossRef]
51. Mizuguchi, N.; Nakata, H.; Hayashi, T.; Sakamoto, M.; Muraoka, T.; Uchida, Y.; Kanosue, K. Brain Activity during Motor Imagery of an Action with an Object: A Functional Magnetic Resonance Imaging Study. *Neurosci. Res.* **2013**, *76*, 150–155. [CrossRef]
52. Lorey, B.; Pilgramm, S.; Bischoff, M.; Stark, R.; Vaitl, D.; Kindermann, S.; Munzert, J.; Zentgraf, K. Activation of the Parieto-Premotor Network Is Associated with Vivid Motor Imagery—A Parametric FMRI Study. *PLoS ONE* **2011**, *6*, e20368. [CrossRef]
53. Chen, Q.; Weidner, R.; Vossel, S.; Weiss, P.H.; Fink, G.R. Neural Mechanisms of Attentional Reorienting in Three-Dimensional Space. *J. Neurosci.* **2012**, *32*, 13352–13362. [CrossRef]

54. Ruggiero, G.; D'Errico, O.; Iachini, T. Development of Egocentric and Allocentric Spatial Representations from Childhood to Elderly Age. *Psychol. Res.* **2016**, *80*, 259–272. [CrossRef] [PubMed]
55. Colombo, D.; Serino, S.; Tuena, C.; Pedroli, E.; Dakanalis, A.; Cipresso, P.; Riva, G. Egocentric and Allocentric Spatial Reference Frames in Aging: A Systematic Review. *Neurosci. Biobehav. Rev.* **2017**, *80*, 605–621. [CrossRef] [PubMed]
56. Moffat, S.D.; Elkins, W.; Resnick, S.M. Age Differences in the Neural Systems Supporting Human Allocentric Spatial Navigation. *Neurobiol. Aging* **2006**, *27*, 965–972. [CrossRef] [PubMed]